

The coupling of the  $^*C-H$  stretch and other  $C-H$  stretching coordinates in **1a** and **1b** is removed by deuteration of their methyl groups. Calculations for **1a-d<sub>6</sub>** and **1b-d<sub>6</sub>** (Table II) also predict large  $^*C-H$  stretching VCD in both conformers. In particular,  $R_{yy}$  is again large in both conformers and larger in **1b-d<sub>6</sub>** than in **1a-d<sub>6</sub>**. We therefore predict that study of the (simpler)  $C-H$  stretching absorption and VCD spectra of **1-d<sub>6</sub>** will yield identical conclusions.

VCD of magnitude comparable to that of the  $^*C-H$  stretch of methyl lactate has been observed in the  $^*C-H$  stretches of similar molecules and attributed to intramolecular ring currents around internally H bonded rings.<sup>1,2</sup> Our results are in direct conflict with these analyses and lead to the conclusion that large methine stretch VCD cannot be uniquely correlated with the presence of a ring. More generally, our results do not support the invocation of the "ring-current mechanism" in the elucidation of the unknown stereochemistry of chiral molecules from their VCD spectra.

**Acknowledgment.** We gratefully acknowledge support by NSF, NIH, NATO, and the San Diego Supercomputer Center.

### Probing Microstructures in Double-Helical DNA with Chiral Metal Complexes: Recognition of Changes in Base-Pair Propeller Twisting in Solution

Anna Marie Pyle,<sup>†</sup> Takashi Morii, and Jacqueline K. Barton\*

*Division of Chemistry and Chemical Engineering, California Institute of Technology, Pasadena, California 91125*

*Received June 5, 1990*

That DNA base pairs are propeller twisted in a sequence-dependent manner has been evident only in viewing crystal structures of oligonucleotides.<sup>1-7</sup> Here we report that shape-selective DNA-binding molecules can recognize and distinguish propeller twisted DNA sites in solution on the basis of shape and symmetry. Enantioselective discrimination is apparent in photocleavage by  $Rh(phen)_2\phi^{3+}$  ( $phen = 1,10$ -phenanthroline;  $\phi = 9,10$ -phenanthrenequinone diimine) at 5'-pyr-pyr-pur-3' steps which are characterized by a high degree of differential propeller twist<sup>8</sup> but not at homopyrimidine-homopurine segments. Neither isomer targets 5'-pur-pyr-3' steps.

Previously we reported that  $Rh(phen)_2\phi^{3+}$ , which binds DNA avidly by intercalation and upon photolysis promotes DNA strand scission, targets DNA sites where the major groove is open and accessible.<sup>9,10</sup> *rac*- $Rh(phen)_2\phi^{3+}$  primarily targets two families

of sequences, 5'-pyr-pyr-pur-3' segments,<sup>2,5,6,11-13</sup> and homopyrimidine sites.<sup>5,14,15</sup> Resolution of  $Rh(phen)_2\phi^{3+}$  into its  $\Delta$  and  $\Lambda$  enantiomers yields mirror-image probes with different specificities for these two target sequences. As can be seen in parts A and B of Figure 1, the  $\Delta$  isomer cleaves strongly at the 5'-CCAG-3' sequences and throughout the homopyrimidine region while both  $\Delta$  and  $\Lambda$  isomers cleave to equivalent extents in the homopyrimidine segments of the fragment. The chiral discrimination evident at 5'-pyr-pyr-pur-3' steps must therefore result from sensing an asymmetry in these steps which is absent at homopyrimidine-homopurine sites.

Cleavage by the enantiomers was next examined on the well-characterized dodecamer<sup>3,13</sup>  $d(CGCGAATTCGCG)_2$  (Figure 1C,D). Here,  $\Delta$ - $Rh(phen)_2\phi^{3+}$  cleaves predominantly at the C9 site whereas the  $\Lambda$  isomer cleaves only weakly at C9. The high level of enantioselectivity is understandable since this C9-G10 step has the highest associated differential propeller twist ( $-11.8^\circ$ ) within the dodecamer. This high differential propeller twist creates a large chiral pocket in the major groove. The cleavage seen at T8 can be accounted for in terms of base tilting ( $1.1^\circ$  at T8 and  $1.6^\circ$  at A17) which opens the major groove,<sup>14</sup> and here, where the differential propeller twist is  $-1.0^\circ$ , there is no associated enantioselectivity. Helical twist provides the only alternate structural parameter which is intrinsically chiral,<sup>16</sup> but helical twisting cannot account for the chiral discrimination observed here. On the basis of the chirality of helical twisting, we would expect<sup>17,18</sup> low enantioselectivity at the C9-G10 step, which is undertwisted ( $32.3^\circ$ ), and high enantioselectivity at the G10-C11 step, which is overtwisted ( $44.7^\circ$ ), contrary to what we observe. Instead, therefore, *the chiral discrimination in site recognition must depend upon the asymmetry associated with propeller twisting.*

It is curious that intercalation which itself produces a structural perturbation at the binding site is still able to sense propeller twisting. Likely the propeller twisting is stabilized by the stacking of purine bases. Perhaps intercalative stacking reinforces this.<sup>19</sup>

The chiral discrimination apparent in the recognition of sites with large differential propeller twist and the absence of such discrimination at homopyrimidine segments which lack differential propeller twisting reflect the different symmetries associated with these steps. The 5'-pyr-pur-3' step, in contrast to the 5'-pyr-pyr-3' step, contains a  $C_2$  axis, the basis for chiral discrimination, perpendicular to the helix along the pseudodyad axis. As shown in Figure 2, the propeller twist of purines at the 5'-pyr-pur-3' site is disposed in an orientation that permits facile intercalation by  $\Delta$ - $Rh(phen)_2\phi^{3+}$ , but the alignment of the ancillary phenanthroline ligands in the  $\Lambda$  isomer, with a contrary orientation

(10) Both spectroscopic analyses on  $\phi$  complexes of ruthenium and product analyses after cleavage by  $\phi$  complexes of rhodium(III) are consistent with a single intercalative interaction in the major groove of the helix. See: Pyle, A. M.; Rehmann, J. P.; Meshoyrer, R.; Kumar, C. V.; Turro, N. J.; Barton, J. K. *J. Am. Chem. Soc.* **1989**, *111*, 3051. Pyle, A. M. Ph.D. Dissertation, Columbia University, 1989. Long, E. C.; Absalon, M. J.; Stubbe, J. A.; Barton, J. K., submitted for publication.

(11) Hunter, W. N.; D'Estaintoto, B. L.; Kennard, O. *Biochemistry* **1989**, *28*, 2444-2451.

(12) Heinemann, U.; Lauble, H.; Frank, R.; Blöcker, H. *Nucleic Acids Res.* **1987**, *15*, 9531-9550.

(13) Dickerson, R.; Drew, H. R. *J. Mol. Biol.* **1981**, *149*, 761-786.

(14) Drew, H. R.; Travers, A. A. *Cell* **1984**, *37*, 491-502.

(15) Ulanovsky, L. E.; Trifonov, E. N. *Nature* **1987**, *326*, 720-722. Marini, J. C.; Levene, S. D.; Crothers, D. M.; Englund, P. T. *Proc. Natl. Acad. Sci. U.S.A.* **1982**, *79*, 7664-7668. Burkhoff, A. M.; Tullius, T. D. *Cell* **1987**, *48*, 935-943. Burkhoff, A. M.; Tullius, T. D. *Nature* **1988**, *331*, 455-457.

(16) Besides this, both the variations in sugar puckering and the rise per base pair also contribute to the opening of the site. These are all, however, not independent parameters. To account for sequence-dependent chiral discrimination, only propeller twisting and helical twisting, the parameters that are asymmetric and potentially sequence dependent, need be considered.

(17) Barton, J. K. *Science* **1986**, *233*, 727-733.

(18) Overall cleavage favors the  $\Delta$  isomer consistent with the right-handed DNA helicity.

(19) Wilson, W. D.; Strekowski, L.; Tanious, F. A.; Watson, R. A.; Mokerosz, J. L.; Strekowska, A.; Webster, G. D.; Neidle, S. *J. Am. Chem. Soc.* **1988**, *110*, 8292-8299.

(20) Maxam, A.; Gilbert, W. *Methods Enzymol.* **1980**, *65*, 499-560.

(21) Dollimore, L. S.; Gillard, R. D. *J. Chem. Soc.* **1973**, 933.

(22) Bosnich, B. *Acc. Chem. Res.* **1969**, *2*, 266.

\* To whom correspondence should be addressed.

<sup>†</sup> Present address: Department of Chemistry and Biochemistry, University of Colorado, Boulder, CO 80309.

(1) Saenger, W. *Principles of Nucleic Acid Structure*; Springer-Verlag: New York, 1984.

(2) Wing, R.; Drew, H.; Takano, T.; Broka, C.; Tanaka, S.; Itakura, K.; Dickerson, R. E. *Nature* **1980**, *287*, 755-758. Wang, A. H.-J.; Fujii, S.; van Boom, J. H.; Rich, A. *Proc. Natl. Acad. Sci. U.S.A.* **1982**, *79*, 3968-3972. Shakked, Z.; Rabinovich, D.; Cruse, W. B. T.; Egert, E.; Kennard, O.; Sala, G.; Salisbury, S. A.; Viswamitra, M. A. *Proc. R. Soc. London, B* **1981**, *231*, 479-487.

(3) Dickerson, R. E. *J. Mol. Biol.* **1983**, *166*, 419-441.

(4) Calladine, C. R. *J. Mol. Biol.* **1982**, *161*, 343-352.

(5) Coll, M.; Frederic, A.; Wang, A. H. J.; Rich, A. *Proc. Natl. Acad. Sci. U.S.A.* **1987**, *84*, 8385-8389. Nelson, H. C.; Finch, J. T.; Luisi, B. F.; Klug, A. *Nature* **1987**, *330*, 221-226.

(6) Timsit, Y.; Westhof, E.; Fuchs, R. P. P.; Moras, D. *Nature* **1989**, *341*, 459-462.

(7) Nadeau, J. G.; Crothers, D. M. *Proc. Natl. Acad. Sci. U.S.A.* **1989**, *86*, 2622-2626. Banks, K. M.; Hare, D. R.; Reid, B. R. *Biochemistry* **1989**, *28*, 6996-7010.

(8) We define differential propeller twist as the angle between the two purine bases projected onto the plane defined by the helical and dyad axes.

(9) Pyle, A. M.; Long, E. C.; Barton, J. K. *J. Am. Chem. Soc.* **1989**, *111*, 4520-4522. Uchida, K.; Pyle, A. M.; Morii, T.; Barton, J. K. *Nucleic Acids Res.* **1989**, *17*, 10259-10265.

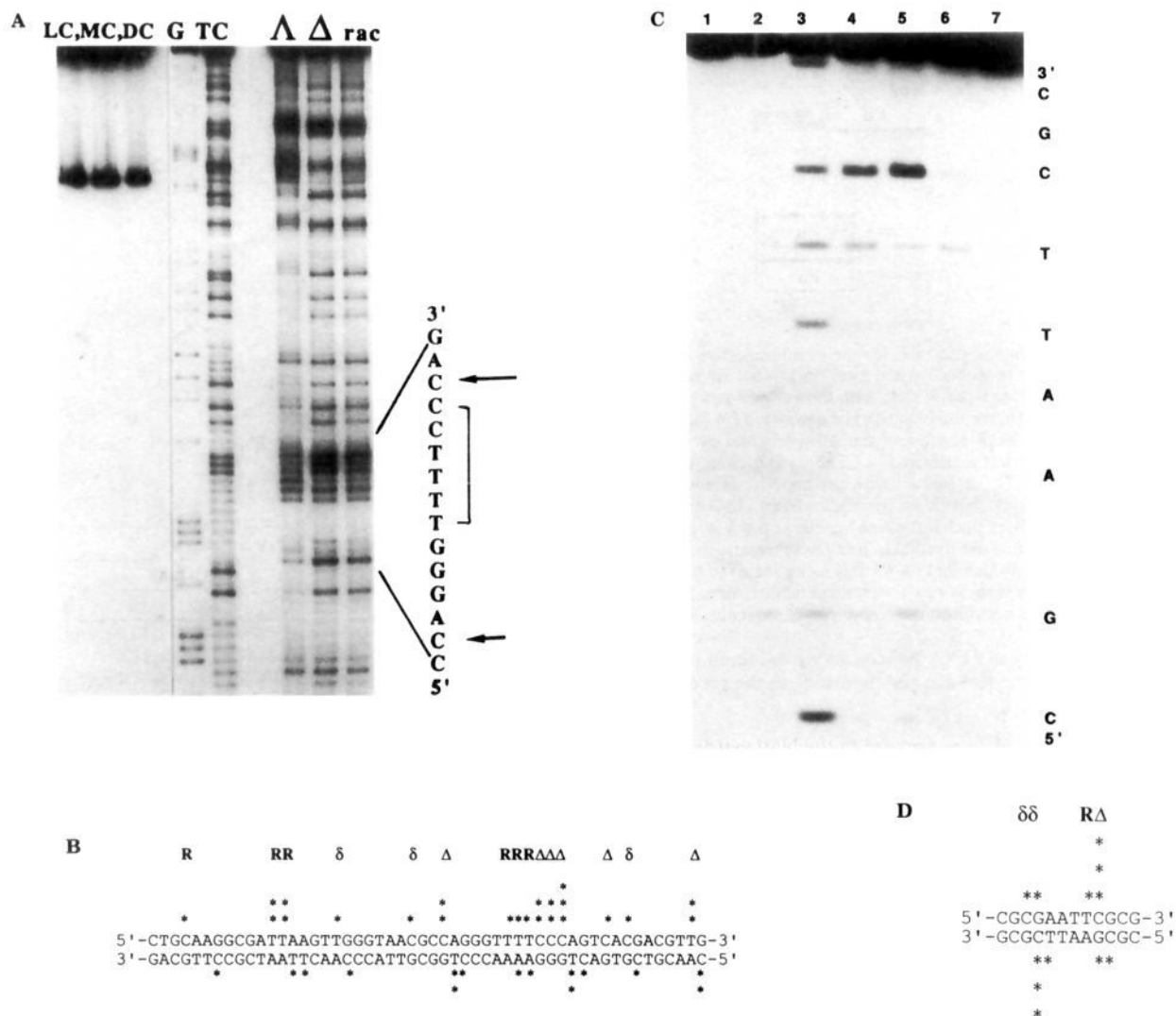


**Figure 1.** (A) Photocleavage by  $\text{Rh}(\text{phen})_2(\text{phi})^{3+}$  enantiomers on a DNA restriction fragment rich in 5'-CCAG-3' sites. The homopyrimidine stretch is marked with a bracket, and the two strongest sites of cleavage by  $\Delta$ - and *rac*- $\text{Rh}(\text{phen})_2(\text{phi})^{3+}$  are indicated with arrows at the right. Also given is the sequence within the marked region. The autoradiograph shows (left to right) lane LC, the light control, irradiation of the fragment for 5 min at 365 nm in the absence of metal complex; lane MC, the metal control, incubation of the DNA with *rac*- $\text{Rh}(\text{phen})_2(\text{phi})^{3+}$  for 5 min in the absence of light; lane DC, the DNA fragment in the absence of metal complex and light; Maxam-Gilbert G reaction;<sup>20</sup> T + C reaction;<sup>20</sup> irradiation for 5 min at 365 nm with 5  $\mu\text{M}$   $\Delta$ - $\text{Rh}(\text{phen})_2(\text{phi})^{3+}$ ;  $\Delta$ - $\text{Rh}(\text{phen})_2(\text{phi})^{3+}$ ; and *rac*- $\text{Rh}(\text{phen})_2(\text{phi})^{3+}$ . Each of the samples contained 50  $\mu\text{M}$  DNA (nucleotides) in tris-acetate buffer (50 mM tris, 20 mM Na acetate, 18 mM NaCl, pH 7.0) and was irradiated with a 1000-W Hg/Xe lamp and monochromator. The DNA fragment was obtained by digestion of pUC19 with *Pvu*II, 5'-end-labeled with [ $\gamma$ -<sup>32</sup>P]ATP and polynucleotide kinase, and a second digestion with *Hind*III. The resultant 144 bp fragments were separated on a non-denaturing polyacrylamide gel and were isolated by electroelution.  $\Delta$ - $\text{Rh}(\text{phen})_2(\text{phi})^{3+}$  was obtained by selective precipitation with potassium (+)-tris[L-cysteinesulphinato]cobaltate(III).<sup>21</sup>  $\Delta\epsilon(\Delta)$  was +138 at 277 nm, and  $\Delta\epsilon(\Delta)$  was -130 at 277 nm. The absolute configuration was assigned by comparison to  $\text{Rh}(\text{phen})_3^{3+}$ , in accordance with exciton chirality theory as described in the literature.<sup>22</sup> (B) Histogram showing the sequence, cleavage pattern, and enantiomeric preferences for the region 330-374 of plasmid pUC19. The cleavage data for the top strand are given in Figure 1A. Cleavage data for the bottom strand are not shown. Stars on the histogram represent relative intensity of cleavage by  $\text{Rh}(\text{phen})_2(\text{phi})^{3+}$  determined on the basis of densitometry.  $\Delta$  represents a large observed chiral selectivity at the site for the  $\Delta$  isomer;  $\delta$  represents a small preference at the site for the  $\Delta$  isomer; and R indicates no appreciable enantiomeric preference. Note the distinct 5'-asymmetry in cleavage, in particular at the pyr-pyr-pur steps with a single base offset. This pattern is consistent both with binding from the major groove and for the pyr-pur steps with the  $C_2$  symmetry characteristic of the step. (C) Photocleavage by  $\text{Rh}(\text{phen})_2(\text{phi})^{3+}$  enantiomers on  $d(\text{CGCGAATTCGCG})_2$  showing the autoradiogram of a 20% denaturing polyacrylamide gel after photocleavage of the 5'-<sup>32</sup>P-labeled dodecamer. Lane 1, fragment in the absence of metal complex and light; lane 2, Maxam-Gilbert<sup>20</sup> G + A reaction; lane 3, C + T reaction;<sup>20</sup> lane 4, fragment after cleavage by *rac*- $\text{Rh}(\text{phen})_2(\text{phi})^{3+}$ ; lane 5,  $\Delta$ - $\text{Rh}(\text{phen})_2(\text{phi})^{3+}$ ; lane 6,  $\Delta$ - $\text{Rh}(\text{phen})_2(\text{phi})^{3+}$ ; lane 7, fragment after irradiation without metal complex. Samples contained 500  $\mu\text{M}$  nucleotide of dodecanucleotide and 25  $\mu\text{M}$  Rh complex in 50 mM sodium cacodylate buffer, pH 7.0. Samples were irradiated at 313 nm for 7.5 min. The dodecamer had been synthesized with a Pharmacia Gene Assembler using the phosphoramidite method and 5'-end-labeled with [ $\gamma$ -<sup>32</sup>P]ATP and T4 polynucleotide kinase. (D) Histogram showing the sequence, cleavage pattern, and enantiomeric preferences on the dodecamer. Symbols are as described in Figure 1B.

clashing with the pyrimidines, precludes similar association. It should be noted that the  $\Delta$  isomer would not be expected to associate preferentially with a 5'-pur-pyr-3' step since in that case the predominant opening arises in the minor groove. Hence it is the consideration of shape that is used in distinguishing between 5'-pur-pyr-3' and 5'-pyr-pur-3' steps.

The chiral discrimination observed here demonstrates that

propeller twisting, evident in crystals, occurs in solution and can serve as an important recognition determinant. Cleavage experiments with these chiral metal complexes now provide a route to examine the sequence dependence of differential propeller twisting in solution on long DNA fragments. Furthermore, just as chiral metal complexes sense the asymmetry in propeller-twisted DNA segments, so too may larger peptide domains. The local

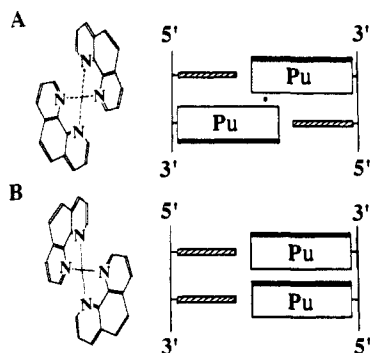


**Figure 2.** An illustration of the basis for the enantioselective cleavage by  $\text{Rh}(\text{phen})_2\text{phi}^{3+}$  at propeller-twisted sites on DNA. Shown schematically in A is the 5'-pyr-pur-3' step, with the purine bases propeller twisted either upward (in the top base pair) or downward (in the bottom base pair), matching the disposition of the  $\Delta$  isomer, and pyrimidines oriented perpendicular to the helical axis. The  $C_2$  axis along the dyad is marked by the  $\bullet$ . The  $\Delta$  isomer, with the opposite orientation of ancillary ligands, would clash with the pyrimidine bases. In B are shown the disposition of ancillary phenanthroline ligands in the  $\Delta$  isomer, also viewed along the intercalative dyad axis, and the schematic illustration of a 5'-pyr-pyr-3' step, which lacks a  $C_2$  axis along the dyad direction. Because of the absence of this  $C_2$  axis, enantiomeric discrimination does not accompany intercalation into the 5'-pyr-pyr-3' sequence.

nucleotide symmetry of DNA helices may provide an indirect, sequence-selective element that is important in the recognition of sites by proteins.

**Acknowledgment.** We are grateful to the National Institutes of Health and the National Foundation for Cancer Research for their financial support. We also thank T. Shields for his excellent technical assistance.

**Registry No.** d(CGCGAATTCGCG), 77889-82-8;  $\Delta$ - $\text{Rh}(\text{phen})_2\text{phi}^{3+}$ , 130192-92-6;  $\Delta$ - $\text{Rh}(\text{phen})_2\text{phi}^{3+}$ , 130192-93-7; *rac*- $\text{Rh}(\text{phen})_2\text{phi}^{3+}$ , 121174-96-7.

**Supplementary Material Available:** An autoradiogram showing cleavage by  $\text{Rh}(\text{phen})_2\text{phi}^{3+}$  enantiomers on a fragment rich in homopyrimidine-homopurine tracts (2 pages). Ordering information is given on any current masthead page.

### Solution Structure of FK 506 from Nuclear Magnetic Resonance and Molecular Dynamics

Peter Karuso,<sup>†</sup> Horst Kessler,\* and Dale F. Mierke

Organisch Chemisches Institut  
Technische Universität München, Lichtenbergstrasse 4  
D-8046 Garching, Federal Republic of Germany

Received July 18, 1990

The conformation of the highly active immunosuppressant FK 506<sup>1-3</sup> (Figure 1) has been examined by high-resolution NMR

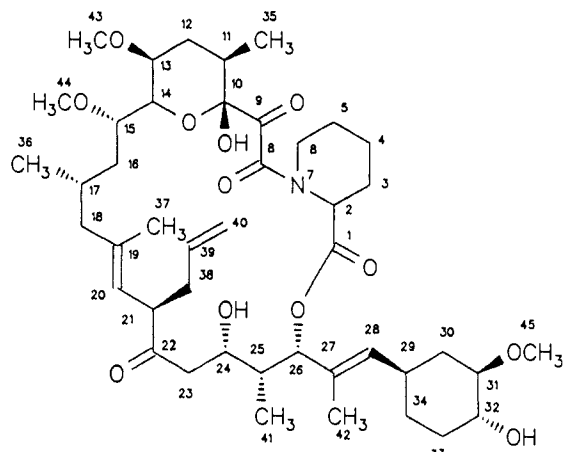


**Figure 1.** Constitution of FK 506 illustrating the numbering of the atoms.

**Table I.** Averages and Standard Deviations of Dihedrals of FK 506 from Molecular Dynamics and X-ray Structure<sup>a</sup>

torsion	cis		trans		X-ray
	av	SD	av	SD	
O2-1-2-3	-63	15	75	33	72
1-2-3-4	-80	7.7	-116	11	-76
2-3-4-5	-51	8.0	-51	8.2	-52
3-4-5-6	51	7.7	58	12	56
4-5-6-N7	-51	8.0	-43	19	-53
5-6-N7-2	53	8.4	47	11	50
6-N7-2-3	-51	7.2	-50	7.6	-47
6-N7-8-9	3	8.3	-178	6.1	1
7-8-9-10	-90	6.9	-98	8.5	-95
8-9-10-11	-47	8.8	134	8.7	-28
9-10-11-12	166	6.9	158	9.0	164
10-11-12-13	-53	6.6	-50	7.3	-54
11-12-13-14	56	5.8	53	7.3	58
12-13-14-15	178	5.8	-173	8.1	-175
13-14-15-16	174	7.4	-175	8.2	-178
14-15-16-17	60	10	58	8.4	68
15-16-17-18	-163	8.5	-140	16	172
16-17-18-19	100	27	151	12	66
17-18-19-20	165	18	174	18	-132
18-19-20-21	174	14	165	12	-168
19-20-21-22	-102	20	-106	16	-141
20-21-22-23	39	40	83	37	137
21-22-23-24	-66	31	-13	46	-118
22-23-24-25	-175	8.3	157	25	59
23-24-25-26	-117	13	73	6.7	-168
24-25-26-27	-89	8.2	177	7.4	56
25-26-27-28	-136	10	-72	8.1	-128
26-27-28-29	180	9.9	176	10	180
27-28-29-30	125	19	116	28	100
28-29-30-31	176	6.9	179	8.2	175
29-30-31-32	-52	6.9	-53	7.6	-56
30-31-32-33	52	7.2	53	7.6	62
31-32-33-34	-52	7.6	-53	7.7	-62
32-33-34-29	53	7.6	53	7.5	59
33-34-29-30	-54	7.2	-53	7.4	-55

<sup>a</sup>The dihedrals are defined by using the numbering of the heavy atoms from the Cambridge Data Bank. The values are given in degrees.

and NOE restrained molecular dynamics simulations. All of the <sup>1</sup>H and <sup>13</sup>C resonances were assigned by using a combination of 2D NMR techniques<sup>4,5</sup> including TOCSY,<sup>6</sup> E. COSY,<sup>7</sup> ROESY,<sup>8</sup>

<sup>†</sup> Present address: School of Chemistry, Macquarie University, Sydney 2109, Australia.

(1) (a) Tanaka, H.; Kuroda, A.; Marusawa, H.; Hatanaka, H.; Kino, T.; Goto, T.; Hashimoto, M. *J. Am. Chem. Soc.* **1987**, *109*, 5031-5033. (b) Kino, T.; Hatanaka, H.; Hashimoto, M.; Goto, T.; Okuhara, M.; Kohsaka, M.; Aoki, H.; Imanaka, H. *J. Antibiot.* **1987**, *40*, 1249-1255. (c) Taga, T.; Tanaka, H.; Goto, T.; Tada, S. *Acta Crystallogr.* **1987**, *C43*, 751-753.

(2) Jones, T. K.; Reamer, R. A.; Desmond, R.; Mills, S. G. *J. Am. Chem. Soc.* **1990**, *112*, 2998-3017.

(3) (a) Starzl, T. E.; Fung, J.; Venkataraman, R.; Todo, S.; Demetris, A. J.; Jain, A. *Lancet* **1989**, 1000-1004. (b) Sickerka, J. J.; Hung, S. H. Y.; Poe, M.; Lin, C. S.; Sigal, N. H. *Nature* **1989**, *341*, 755-757. (c) Harding, M. W.; Galat, A.; Uehling, D. E.; Schreiber, S. L. *Nature* **1989**, *341*, 758-760. (d) Freedman, R. B. *Nature* **1989**, *341*, 692.

(4) All NMR spectra were recorded at -30 or 27 °C on an AMX 600 (600 MHz) spectrometer equipped with ASPECT X32 and 3000 computers. A sample of FK 506 (20 mg) was dissolved in 0.5 mL of deuterated chloroform to give a final concentration of approximately 25 mM for each of the two configurational isomers.

(5) Kessler, H.; Gehrke, M.; Griesinger, C. *Angew. Chem.* **1988**, *100*, 507-554; *Angew. Chem., Int. Ed. Engl.* **1988**, *27*, 490-536.

(6) (a) Braunschweiler, L.; Ernst, R. R. *J. Magn. Reson.* **1983**, *53*, 521-528. (b) Davis, D. G.; Bax, A. *J. Am. Chem. Soc.* **1985**, *107*, 2820-2821.